

Analysis, modeling and optimal control of COVID-19 outbreak with three forms of infection in Democratic Republic of the Congo

A.M. Ndondo^{a,d,h}, S.K. Kasereka^{b,d,*}, S.F. Bisuta^{c,d}, K. Kyamakya^e, E.F.G. Doungmo^f, R-B. M. Ngoie^g

^a University of Lubumbashi, Mathematics and Computer Science Department, Lubumbashi, Democratic Republic of the Congo

^b University of Kinshasa, Mathematics and Computer Science Department, Kinshasa, Democratic Republic of the Congo

^c University of Kinshasa, Pneumology Department, University Clinics of Kinshasa, Democratic Republic of the Congo

^d Artificial intelligence, Big data and modeling simulation Research Center (ABIL), Kinshasa, Democratic Republic of the Congo

^e Alpen-Adria-Universität Klagenfurt, Institute of Smart Systems Technologies, Department of Mathematical Sciences, Klagenfurt, Austria

^f University of South Africa, College of Science, Engineering & Technology, Department of Mathematical Sciences, Florida 003, South Africa

^g Institut Supérieur Pédagogique, Department of Mathematics, Mbanza-Ngungu, Congo

^h Université Nouveaux Horizons, Faculty of Computer Science, Lubumbashi, Democratic Republic of the Congo

ARTICLE INFO

Keywords:

COVID-19
Mathematical model
Simulation
Optimal control
DRC
Differential equation

ABSTRACT

This paper deals with modeling and simulation of the novel coronavirus in which the infectious individuals are divided into three subgroups representing three forms of infection. The rigorous analysis of the mathematical model is provided. We provide also a rigorous derivation of the basic reproduction number \mathcal{R}_0 . For $\mathcal{R}_0 < 1$, we prove that the Disease Free Equilibrium (DFE) is Globally Asymptotically Stable (GAS), thus COVID-19 extincts; whereas for $\mathcal{R}_0 > 1$, we found the co-existing phenomena under some assumptions and parametric values. Elasticity indices for \mathcal{R}_0 with respect to different parameters are calculated with baseline parameter values estimated. We also prove that a transcritical bifurcation occurs at $\mathcal{R}_0 = 1$. Taking into account the control strategies like screening, treatment and isolation (social distancing measures), we present the optimal control problem of minimizing the cost due to the application of these measures. By reducing the values of some parameters, such as death rates (representing a management effort for all categories of people) and recovered rates (representing the action of reduction in transmission, improved screening, treatment for individuals diagnosed positive to COVID-19 and the implementation of barrier measures limiting contamination for undiagnosed individuals), it appears that after 140–170 days, the peak of the pandemic is reached and shows that by continuing with this strategy, COVID-19 could be eliminated in the population.

Introduction

Since the last quarter of 2019, a deadly pandemic of rapid evolution, COVID-19 (SARS-CoV-2) has spread around the world. The acronym refers to Severe Acute Respiratory Syndrome in reference to the previous 2003 epidemic caused by a related coronavirus. This disease is so contagious that it affects the respiratory tract. It is transmitted from animal (host) to animal (intermediate host), intermediate host to human and human to human. A pandemic occurs when a new virus spreads around the world. As long as people are less protected against this new virus, they are more prone to be sick. Its transmission is spread through the droplets of an infected person when he cough, sneez, sing, speak, breath heavily etc. which are sprayed in the air. This COVID-19 can also be

spread after infected people sneeze, cough or touch surfaces or objects. Other people may become infected by being in close or direct contact with the infected people or by touching contaminated surfaces or objects then touch their eyes, noses or mouths prior to cleaning their hands [1,2]. Normally, the symptoms develop on an average of 5 to 7 days after contamination, with extremes ranging from 2 to 12 days. For precaution, a period of 14 days is considered for isolation. To fully understand the mechanisms of this invisible transmission, a distinction must be made between incubation, the period between the initial encounter with the virus and the appearance of the first symptoms; and contagiousness, the period during which a person can transmit the disease. According to a Chinese study of 191 patients, the incubation period is on average two days with extremes ranging from 0 to 24 days, and contagiousness is

* Corresponding author at: University of Kinshasa, Mathematics and Computer Science Department, Kinshasa, Democratic Republic of the Congo.

E-mail address: selain.kasereka@unikin.ac.cd (S.K. Kasereka).

<https://doi.org/10.1016/j.rinp.2021.104096>

Received 11 November 2020; Received in revised form 2 March 2021; Accepted 16 March 2021

Available online 27 March 2021

2211-3797/© 2021 The Author(s).

Published by Elsevier B.V. This is an open access article under the CC BY-NC-ND license

(<http://creativecommons.org/licenses/by-nc-nd/4.0/>).

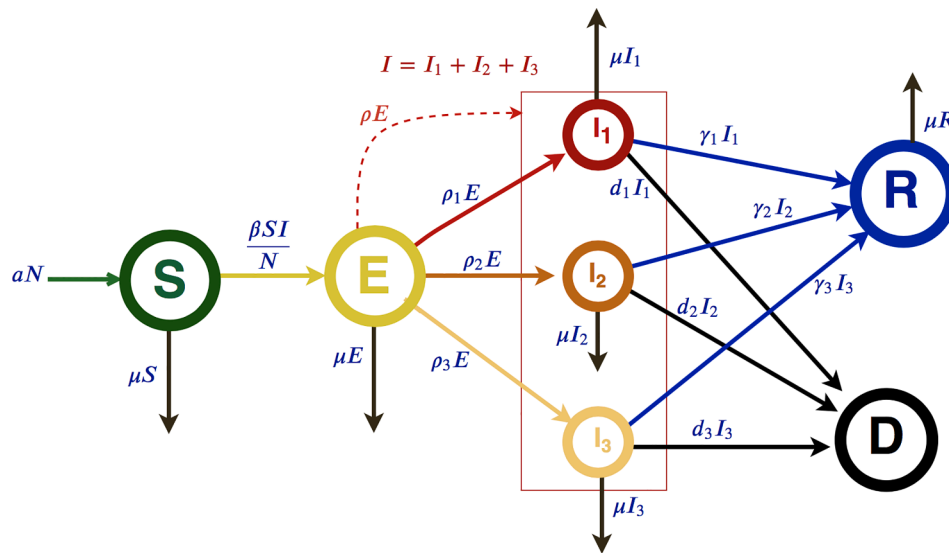


Fig. 1. Transfer diagram describing the COVID-19 dynamics.

about 20 days after the onset of clinical signs – whether symptomatic or not – with a maximum of 37 days [3].

In Europe, researchers estimated that COVID-19 was introduced into France “around mid-January”. However, this estimation is somewhat fragile insofar as the diversity observed between the sequenced viral strains is very low and researchers currently have only a small number of representative samples from different regions of France [4]. Individuals of 70 years and older [5] infected with COVID-19 and having a chronic heart disease, chronic lung disease, cancer and immunodeficiency, and diabetes are at risk of death. But currently the mechanisms linked to thromboembolic disease seem to be the most incriminated and are increasingly known [6,7].

COVID-19 can circulate *incognito*. Understanding the mechanisms of its transmission by people with no symptoms is essential. Symptomless infected people, unaware that they are infected, so they do not protect themselves and tend to unintentionally infect others repeatedly.

The basic reproduction number (\mathcal{R}_0) is essential for modelling the evolution of the disease as it is done in [8]. This number depends on the population density, the average duration of infection and the ease with which the virus is transmitted. In order to assess it, investigations must be carried out: we try to go up to the chain of transmission. The aim is to find out who was infected by whom, mentioned an Asian study [9]. The time that elapses between the onset of symptoms in an infectious person and the onset of symptoms in an infected person is still much debated. A new American study puts it at 7 or 8 days (compared to 4.6 days in the Chinese study). This in comparison with the values of R_0 in the USA and in China oscillating from 2 to 4 as reported in [10].

The first positive case of COVID-19 in Democratic Republic of the Congo (DRC) was detected on 10 March 2020, and after 6 weeks the country counted already 400 positive patients and after 3 months more than 5000 cases [11]. Several scenarios have been proposed to reflect the evolution of this disease in the world and in some countries. The research’s question was to know what was the main reason of the evolution of this disease in DRC. The simulations were carried out in two stages, during the upward and downward slopes of the epidemic. The profile of the index case would have an influence on the contact cases, so discussions are still opened on this subject. One team argued that it would make no difference and a more recent study supports arguments to the contrary [10], they showed that asymptomatic people would have lower transmissibility.

Several mathematical models have been developed by researchers in an attempt to control the spread of infectious diseases in general [12–18] and COVID-19 in particular. More recently [19] proposed and

analyzed compartmental model of Covid-19 to predict and control the pandemic. [20] presented mathematical results of a fractional model considering that the seafood market is an important source for COVID-19 infection. [21] presented a mathematical model by identifying the endemicity parameters of COVID-19 and determine which parameter is the most dominant to affect the disease endemicity. [22] proposed a model based on Atangana-Baleanu-Caputo (ABC) derivative with two compartments (healthy and infected). [23] proposed a model based on fixed point and establish related existence results under ABC derivative with fractional order. [24] studied a mathematical model based on a fractional Atangana-Baleanu (AB) operator. [25] presented a model with three compartments (susceptible, infected and recovered) which is extended into a stochastic model in [26]. A model with four compartments (susceptible, exposed, infected and recovered) is discussed in [27].

Unfortunately, most mathematical models of COVID-19 consider that all individuals, regardless of age, are susceptible to the same form of COVID-19 infection and all infected individuals have the same cure rate in the population. In this paper, we propose a mathematical model which assume that it would have differences, so the infected individuals were divided into 3 groups; (1) people with a low risk of developing complications, most of whom are asymptomatic carriers, in our case it was assimilated to young people; (2) people with a moderate risk of developing severe symptomatology, and (3) those with a high risk of developing complications with a high death rate. In addition, they are also those who have a high proportion of comorbidity. Congolese population configuration is a broad-based pyramid while the western and industrialized countries configuration is narrowed with a flared top reflecting a large proportion of elderly people.

This paper is structured as follow: Firstly we present the model description. Secondly we show the mathematical analysis of model proposed. Thirdly we present the elasticity indices of the basic reproduction number \mathcal{R}_0 with respect to the model parameters. Fourthly we discuss the optimal control problem of the model and finally some numerical simulations are presented before discussing the obtained results.

Description of the model and settings

A compartmental model of COVID-19

Let us consider N as the total population and assume that anyone is susceptible to catch COVID-19. N is composed by seven compartments S, E, I_1, I_2, I_3, R and D which represent respectively susceptible, exposed,

Table 1
Parameters description, meaning and estimated baseline values.

Parameters	Meaning	Estimated baseline values
a	Recruitment rate	0.304
β	Transmission rate	0.3
ρ_1	Progression rate from E to I_1	0.575
ρ_2	Progression rate from E to I_2	0.377
ρ_3	Progression rate from E to I_3	0.048
μ	Natural mortality rate	1.92×10^{-2}
d_1	Mortality rate due to COVID-19 for I_1	10^{-4}
d_2	Mortality rate due to COVID-19 for I_2	5×10^{-4}
d_3	Mortality rate due to COVID-19 for I_3	0.20
γ_1	Recovered rate for I_1	0.025
γ_2	Recovered rate for I_2	1.25×10^{-2}
γ_3	Recovered rate for I_3	625×10^{-5}

infectious benign form (young people), infectious respiratory form (adults people), infectious reanimator form (old and comorbidity people), recovered and COVID-19 deaths. We note by a, μ and d respectively the birth rate, the natural mortality rate and the mortality rate due to COVID-19. Susceptible S will be exposed if they are in contact with infectious persons (I_1, I_2 and I_3) at a transmission rate β . Exposed individuals will progress to the infectious compartment I according to the rates ρ_1 for form I_1, ρ_2 for form I_2 and ρ_3 for form I_3 . Infectious individuals can be removed according to the rates γ_1 for I_1 form, γ_2 for I_2 form and γ_3 for I_3 form. The mortality rates due to COVID-19 for individuals I_1, I_2 and I_3 are denoted by d_1, d_2 and d_3 respectively. We assume that $I = I_1 + I_2 + I_3$. The dynamics of Coronavirus transmission are shown in Fig. 1.

Based on Fig. 1 we obtain the equation system (1).

$$\begin{cases} \dot{S} = aN - \beta \frac{S(t)I(t)}{N} - \mu S(t), \\ \dot{E} = \beta \frac{S(t)I(t)}{N} - (\rho_1 + \rho_2 + \rho_3 + \mu)E(t), \\ \dot{I}_1 = \rho_1 E(t) - (\mu + \gamma_1 + d_1)I_1(t), \\ \dot{I}_2 = \rho_2 E(t) - (\mu + \gamma_2 + d_2)I_2(t), \\ \dot{I}_3 = \rho_3 E(t) - (\mu + \gamma_3 + d_3)I_3(t), \\ \dot{R} = \sum_{i=1}^3 \gamma_i I_i(t) - \mu R(t), \\ \dot{D} = \sum_{i=1}^3 d_i I_i(t), \\ I = \sum_{i=1}^3 I_i(t), \\ N = S + E + I_1 + I_2 + I_3 + R + D. \end{cases} \tag{1}$$

By dividing all terms of system (1) by N , we define $s = \frac{S}{N}; e = \frac{E}{N}; i = \frac{I}{N};$
 $d = \frac{D}{N}$ and $r = \frac{R}{N}$ we obtain the equation system (2):

$$\begin{cases} \dot{s} = a - \beta si - \mu s, \\ \dot{e} = \beta si - (\rho_1 + \rho_2 + \rho_3 + \mu)e, \\ \dot{i}_k = \rho_k e - (\mu + \gamma_k)i_k, \\ \dot{r} = \sum_{k=1}^3 \gamma_k i_k - \mu r, \\ \dot{d} = \sum_{k=1}^3 d_k i_k, \\ \dot{i} = \sum_{k=1}^3 i_k. \end{cases} \tag{2}$$

With $s + e + i_1 + i_2 + i_3 + r + d = 1$ and $\rho_1 + \rho_2 + \rho_3 = 1$. Then $s, e, i_k, r,$
 d with $k = 1, 2, 3$ represent the proportions and take values in the closed interval $[0, 1]$.

Model parameters

Parameters used in this paper were taken from the literature or based on reported data from DRC. Table 1 presents description, meaning and estimated baseline values of all used parameters.

Mathematical analysis

Positivity and boundedness of the solution

This subsection is provided to prove the positivity and boundedness of solutions of the system (2) with initial condition $(s(0), e(0), i_1(0), i_2(0), i_3(0), r(0), d(0))^T \in [0, 1]^7$.

Lemma 0.1. Suppose $\Omega \subset [0, 1] \times \mathbb{C}^n$ is open, $f_i \in C(\Omega, [0, 1]),$
 $i = 1, 2, \dots, n$. If $f_i|_{x_i(t)=0}, X_t \in \mathbb{C}_{+0}^n \geq 0, X_t = (x_{1t}, x_{2t}, \dots, x_{nt})^T, i = 1,$
 $2, \dots, n$. Then $\mathbb{C}_{+0}^n \{ \phi_1, \phi_2, \dots, \phi_n \} : \phi \in \mathbb{C}([-\tau, 0], [0, 1]^n)$ is the invariant domain of the following equations: $\frac{dx_i(t)}{dt} = f_i(t, X_t), t \geq \tau, i = 1, 2, \dots, n$ where $[0, 1]^n = \{ (x_1, x_2, \dots, x_n) : x_i \geq 0, i = 1, n \} [1]$.

Proposition 0.2. The system (2) is invariant in $[0, 1]^7$.

Proof. By re-writing the system (2) we have:

$$\frac{dX}{dt} = M(X(t)); X(0) = X_0 \geq 0 \text{ with } M(X(t)) = (M_1(X), M_2(X), \dots, M_7(X))^T$$

$M(x(t)) = (M_1(x), M_2(x), \dots, M_7(x)).$ we note that: $\left. \frac{ds}{dt} \right|_{s=0} = a \in [0,$
 $1] \left. \frac{de}{dt} \right|_{e=0} = \rho_k e \in [0, 1] \left. \frac{de}{dt} \right|_{e=0} = \beta si \in [0, 1] \left. \frac{dr}{dt} \right|_{r=0} = \sum_{k=1}^3 \gamma_k i_k \in [0,$
 $1] \left. \frac{dd}{dt} \right|_{d=0} = \sum_{k=1}^3 d_k i_k \in [0, 1]$ Then it follows from the Lemma 0.1 that is an invariant set $[0, 1]^7$. \square

Proposition 0.3. The system (2) is bounded in the region

$$\Omega = (s, e, i_1, i_2, i_3, r, d) \in [0, 1]^7, s + e + i_1 + i_2 + i_3 + r + d \leq \frac{a}{\mu}$$

Proof. From the system (2) we observed that

$$\frac{dn}{dt} = a - \mu n$$

$$n(t) = \frac{a}{\mu} + Ke^{-\mu t}$$

with $K \in \mathbb{R}$, an integration constant.

$$\lim_{t \rightarrow +\infty} \sup n(t) = \frac{a}{\mu}$$

Hence the system (2) is bounded. \square

Diseases Free Equilibrium and basic reproduction number

The Diseases Free equilibrium (DFE) is obtained for the system (2) by supposing $e = i_1 = i_2 = i_3 = r = d = 0$ which is denoted by

$$X_0^* = \left(s^* = \frac{a}{\mu}, 0, 0, 0, 0, 0 \right)$$

By using the next generation method as applied in [28,29], we find the reproduction number denoted by \mathcal{R}_0 . For that, we consider only the compartments which are infected from the system (2) and decompose the right hand side as $\mathcal{F} - \mathcal{V}$, where \mathcal{F} is the transmission part, expressing the production of the new infection, and the transition part is \mathcal{V} , which describe the change in state:

$$\mathcal{F} = \begin{pmatrix} \beta(i_1 + i_2 + i_3)s \\ 0 \\ 0 \\ 0 \\ 0 \end{pmatrix}; \mathcal{V} = \begin{pmatrix} (\rho_2 + \rho_3 + \mu)e \\ \rho_1 e + (\mu + \gamma_1 + d_1)i_1 \\ \rho_2 e + (\mu + \gamma_2 + d_2)i_2 \\ \rho_3 e + (\mu + \gamma_3 + d_3)i_3 \\ \gamma_1 i_1 + \gamma_2 i_2 + \gamma_3 i_3 + \mu r \end{pmatrix}$$

The Jacobian of \mathcal{F} and \mathcal{V} at the DFE X_0^* give

$$F = \begin{pmatrix} 0 & \frac{a}{\mu}\beta & \frac{a}{\mu}\beta & \frac{a}{\mu}\beta \\ 0 & 0 & 0 & 0 \\ 0 & 0 & 0 & 0 \\ 0 & 0 & 0 & 0 \end{pmatrix}, V = \begin{pmatrix} \rho_1 + \rho_2 + \rho_3 + \mu & 0 & 0 & 0 \\ \rho_1 & \mu + \gamma_1 + d_1 & 0 & 0 \\ \rho_2 & 0 & \mu + \gamma_2 + d_2 & 0 \\ \rho_3 & 0 & 0 & \mu + \gamma_3 + d_3 \end{pmatrix}$$

Following [28], $\mathcal{R}_0 = \rho(-FV^{-1})$, where ρ is the spectral radius of the next-generation matrix $(-FV^{-1})$.

Thus, from the system (2), we have:

$$\mathcal{R}_0 = \frac{a\beta}{\mu(\rho_1 + \rho_2 + \rho_3 + \mu)} \left(\frac{\rho_1}{\mu + \gamma_1 + d_1} + \frac{\rho_2}{\mu + \gamma_2 + d_2} + \frac{\rho_3}{\mu + \gamma_3 + d_3} \right) \quad (3)$$

Stability of the diseases free equilibrium

aaa

Theorem 0.4. *The disease free equilibrium (DFE) $X_0^* = \left(\frac{a}{\mu}, 0, 0, 0, 0, 0 \right)$ of the system (2) is locally stable if $\mathcal{R}_0 < 1$ and unstable if $\mathcal{R}_0 > 1$*

Proof. From the model system (2), the Jacobian at DFE is given by:

$$J_{X_0^*} = \begin{pmatrix} -\mu & 0 & \frac{-a\beta}{\mu} & \frac{-a\beta}{\mu} & \frac{-a\beta}{\mu} & 0 \\ 0 & -\rho_1 - \rho_2 - \rho_3 - \mu & \frac{a\beta}{\mu} & \frac{a\beta}{\mu} & \frac{a\beta}{\mu} & 0 \\ 0 & \rho_1 & -\mu - \gamma_1 - d_1 & 0 & 0 & 0 \\ 0 & \rho_2 & 0 & -\mu - \gamma_2 - d_2 & 0 & 0 \\ 0 & \rho_3 & 0 & 0 & -\mu - \gamma_3 - d_3 & 0 \\ 0 & 0 & \gamma_1 & \gamma_2 & \gamma_3 & -\mu \end{pmatrix}$$

To define the characteristic equation, we note λ as the eigenvalue of the matrix $J_{X_0^*}$. We obtain the following result:

$$Det(J_{X_0^*} - \lambda I) = 0$$

$$\Rightarrow (\lambda + \mu)^2 - \rho_1 \left(\frac{a\beta}{\mu} \right) (\mu + \gamma_2 + \lambda) (\mu + \gamma_3 + \lambda) - (\mu + \gamma_1 + \lambda) \left[\rho_2 \left(\frac{a\beta}{\mu} \right) (\mu + \gamma_3 + \lambda) - Z + (\mu + \gamma_2 + \lambda) \left(\frac{a\beta}{\mu} \right) \rho_3 \right] = 0$$

Where $Z = (\mu + \gamma_2 + \lambda)(\rho_1 + \rho_2 + \mu + \lambda)(\mu + \gamma_3 + \lambda)$.

$$\Rightarrow \frac{-a\beta}{\mu} \rho_1 (\mu + \gamma_2 + d_2 + \lambda) (\mu + \gamma_3 + d_3 + \lambda) + (-\mu - \gamma_1 - d_1 - \lambda) (-\rho_1 - \rho_2 - \rho_3 - \mu - \lambda) (\mu + \gamma_2 + d_2 + \lambda) (\mu + \gamma_3 + d_3 + \lambda) + \frac{a\beta}{\mu} \rho_3 (\mu + \gamma_2 + d_2 + \lambda) + \frac{a\beta}{\mu} \rho_2 (\mu + \gamma_3 + d_3 + \lambda) = 0$$

$$\Rightarrow \frac{-a\beta}{\mu} \rho_1 (\mu + \gamma_2 + d_2 + \lambda) (\mu + \gamma_3 + d_3 + \lambda) - (\mu + \gamma_1 + d_1 + \lambda) (\rho_1 + \rho_2 + \rho_3 + \mu + \lambda) (\mu + \gamma_2 + d_2 + \lambda) (\mu + \gamma_3 + d_3 + \lambda) + \frac{a\beta}{\mu} \rho_3 (\mu + \gamma_2 + d_2 + \lambda) + \frac{a\beta}{\mu} \rho_2 (\mu + \gamma_3 + d_3 + \lambda) = 0$$

$$\Rightarrow \frac{a\beta}{\mu} [\rho_1 (\mu + \gamma_2 + d_2 + \lambda) (\mu + \gamma_3 + d_3 + \lambda) + \rho_2 (\mu + \gamma_1 + d_1 + \lambda) (\mu + \gamma_3 + d_3 + \lambda) + \rho_3 (\mu + \gamma_1 + d_1 + \lambda) (\mu + \gamma_2 + d_2 + \lambda)] = (\mu + \gamma_1 + d_1 + \lambda) (\rho_1 + \rho_2 + \rho_3 + \mu + \lambda) (\mu + \gamma_2 + d_2 + \lambda) (\mu + \gamma_3 + d_3 + \lambda)$$

$$\Rightarrow \frac{a\beta}{\mu} \left[\frac{\rho_1}{(\mu + \gamma_1 + d_1 + \lambda) (\rho_1 + \rho_2 + \rho_3 + \mu + \lambda)} + \frac{\rho_2}{(\rho_1 + \rho_2 + \rho_3 + \mu + \lambda) (\mu + \gamma_2 + d_2 + \lambda)} + \frac{\rho_3}{(\rho_1 + \rho_2 + \rho_3 + \mu + \lambda) (\mu + \gamma_3 + d_3 + \lambda)} \right] = 1$$

$$\Rightarrow \frac{a\beta}{\mu(\rho_1 + \rho_2 + \rho_3)} \left[\frac{\rho_1}{\mu + \gamma_1 + d_1 + \lambda} + \frac{\rho_2}{\mu + \gamma_2 + d_2 + \lambda} + \frac{\rho_3}{\mu + \gamma_3 + d_3 + \lambda} \right] = 1$$

Denote

$$G_1(\lambda) = \frac{a\beta\rho_1}{\mu(\rho_1 + \rho_2 + \rho_3 + \mu + \lambda)(\mu + \gamma_1 + d_1 + \lambda)} + \frac{a\beta\rho_2}{\mu(\rho_1 + \rho_2 + \rho_3 + \mu + \lambda)(\mu + \gamma_2 + d_2 + \lambda)} + \frac{a\beta\rho_3}{\mu(\rho_1 + \rho_2 + \rho_3 + \mu + \lambda)(\mu + \gamma_3 + d_3 + \lambda)}$$

We rewrite $G_1(\lambda)$ as $G_1(\lambda) = G_{11}(\lambda) + G_{12}(\lambda) + G_{13}(\lambda)$.

Now if $\text{Re}(\lambda) \geq 0, \lambda = x + iy$, then $|G_{11}(\lambda)| \leq G_{11}(x) \leq G_{11}(0)$

$$|G_{11}(\lambda)| \leq \frac{a\beta\rho_1}{\mu|\rho_1 + \rho_2 + \rho_3 + \mu + \lambda||\mu + \rho_1 + d_1 + \lambda|} \leq G_{11}(x) \leq G_{11}(0)$$

$$|G_{12}(\lambda)| \leq \frac{a\beta\rho_2}{\mu|\rho_1 + \rho_2 + \rho_3 + \mu + \lambda||\mu + \rho_2 + d_2 + \lambda|} \leq G_{12}(x) \leq G_{12}(0)$$

$$|G_{13}(\lambda)| \leq \frac{a\beta\rho_3}{\mu|\rho_1 + \rho_2 + \rho_3 + \mu + \lambda||\mu + \rho_3 + d_3 + \lambda|} \leq G_{13}(x) \leq G_{13}(0)$$

Then

$$G_{11}(0) + G_{12}(0) + G_{13}(0) = G_1(0) = R_0 < 1,$$

which implies

$$|G_1(\lambda)| \leq 1$$

Thus for $R_0 < 1$, we can found that all λ of the characteristics equation $G_1(\lambda) = 1$ has negative real parts.

As a consequence, if $R_0 < 1$, all λ are negatives and the DFE noted by X_0^* is locally asymptotically stable.

Now, by considering $R_0 > 1$, that is mean $G_1(0) > 1$, then

$$\lim_{\lambda \rightarrow \infty} G_1(\lambda) = 0$$

Then there exists $\lambda_1^* > 0$ such that $G_1(\lambda_1^*) = 1$. This imply that there exist positive eigenvalue ($\lambda_1^* > 0$) of $J_{X_0^*}$. Hence X_0^* is unstable whenever $R_0 > 1$. \square

Theorem 0.5. *The disease free equilibrium (DFE) $X_0^* = (\frac{a}{\mu}, 0, 0, 0, 0, 0)$ of the equation system (2) is globally asymptotically stable (GAS) if $R_0 < 1$ and unstable if $R_0 > 1$.*

Rewriting the equation system (2) as

$$\begin{cases} \frac{dX}{dt} = F(X, V) \\ \frac{dV}{dt} = G(X, V), \text{ with } G(X, 0) = 0 \end{cases} \quad (4)$$

$$D_V G(X^*, 0) = \begin{pmatrix} -(\rho_1 + \rho_2 + \rho_3 + \mu) & \frac{a\beta}{\mu} & \frac{a\beta}{\mu} & \frac{a\beta}{\mu} \\ \rho_1 & -(\mu + \gamma_1 + d_1) & 0 & 0 \\ \rho_2 & 0 & -(\mu + \rho_2 + d_2) & 0 \\ \rho_3 & 0 & 0 & -(\mu + \rho_3 + d_3) \end{pmatrix}$$

where $X = (s, r) \in [0, 1]^2$ (proportions of uninfected individuals), $V = (e, i_1, i_2, i_3) \in [0, 1]^4$ (proportions of infected individuals) and $X_0^* = (\frac{a}{\mu}, 0, 0, 0, 0, 0)$ is the DFE of the system (2). The global stability of the DFE is guaranteed if those two conditions are satisfied:

1. For $\frac{dx}{dt} = F(X, 0), X^*$ is globally asymptotically stable,
2. $G(X, V) = AV - \widehat{G}(X, V); \widehat{G}(X, V) \geq 0$ for $(X, V) \in [0, 1]^6$ where $A = D_V G(X^*, 0)$ is a metzler matrix and $[0, 1]^6$ is the positive invariant set with respect to the model (2).

Following [30] we check the conditions mentioned above:

$$\frac{dx}{dt} = F(X, I) = \begin{cases} a - \beta si_1 - \beta si_2 - \beta si_3 - \mu s \\ \gamma_1 i_1 + \gamma_2 i_2 + \gamma_3 i_3 - \mu r \end{cases}$$

$$\frac{dI}{dt} = G(X, I) = \begin{cases} \beta si_1 - \beta si_2 - \beta si_3 - (\rho_1 + \rho_2 + \rho_3 + \mu)e \\ \rho_1 e - (\mu + \gamma_1 + d_1)i_1 \\ \rho_2 e - (\mu + \gamma_2 + d_2)i_2 \\ \rho_3 e - (\mu + \gamma_3 + d_3)i_3 \end{cases}$$

$$G(X, 0) = 0, U_0 = (X_0^*) = (\frac{a}{\mu}, 0, 0, 0, 0, 0).$$

The conditions (H_1) and (H_2) below must be met in order to guarantee the local asymptotic stability.

(H_1) for $\frac{dx}{dt} = F(X, 0), X_0^*$ is global asymptotically stable (GAS).

(H_2) $G(X, I) = AI - \widehat{G}(X, I); \widehat{G}(X, I) \geq 0$ for $(X, I) \in \Omega$ where $A = D_V G(X^*, 0)$ is an M-matrix, the off diagonal element of A are non negative and Ω is the region where the model makes biological sense.

For the equation system (2), we have:

$$F(X, 0) = \begin{pmatrix} a - \mu s \\ 0 \end{pmatrix},$$

and

$$G(X, I) = \begin{cases} \beta si_1 - \beta si_2 - \beta si_3 - (\rho_1 + \rho_2 + \rho_3 + \mu)e \\ \rho_1 e - (\mu + \gamma_1 + d_1)i_1 \\ \rho_2 e - (\mu + \gamma_2 + d_2)i_2 \\ \rho_3 e - (\mu + \gamma_3 + d_3)i_3 \end{cases}$$

Then,

We deduce

$$i_1^* = \frac{a\rho_1}{(\rho_1+\rho_2+\rho_3+\mu)(\mu+\gamma_1+d_1)} \left[1 - \frac{1}{\mathcal{R}_0} \right]$$

$$A = \begin{pmatrix} -(\rho_1 + \rho_2 + \rho_3 + \mu) \frac{a\beta}{\mu} & \frac{a\beta}{\mu} & \frac{a\beta}{\mu} & \frac{a\beta}{\mu} \\ \rho_1 & -(\mu + \gamma_1 + d_1) & 0 & 0 \\ \rho_2 & 0 & -(\mu + \rho_2 + d_2) & 0 \\ \rho_3 & 0 & 0 & -(\mu + \rho_3 + d_3) \end{pmatrix}$$

$$AI = \begin{pmatrix} -(\rho_1 + \rho_2 + \rho_3 + \mu)e + \frac{a\beta}{\mu} + \frac{a\beta}{\mu} + \frac{a\beta}{\mu} \\ \rho_1 e - (\mu + \gamma_1 + d_1)i_1 \\ \rho_2 e - (\mu + \rho_2 + d_2)i_2 \\ \rho_3 e - (\mu + \rho_3 + d_3)i_3 \end{pmatrix}$$

and

$$\tilde{G}(X, I) = \begin{pmatrix} \beta(i_1 + i_2 + i_3) \left(\frac{a}{\mu} - s \right) \\ 0 \end{pmatrix}$$

Clearly, $\tilde{G}(X, I) \geq 0$ whenever the state variables are inside Ω as $\left(\frac{a}{\mu} - s \right) > 0$.

Also, it is clear that $X_0^* = \left(\frac{a}{\mu}, 0, 0, 0, 0, 0, 0 \right)$ is a globally asymptotically stable equilibrium of the system $\frac{dX}{dt} = F(X, 0)$.

Hence, the [Theorem 0.5](#) holds.

Existence and co-existing equilibrium point

In this subsection, the existence and the local stability of the co-

$$J_{X_0^*} = \begin{pmatrix} -\mu & 0 & \frac{-a\beta}{\mu} & \frac{-a\beta}{\mu} & \frac{-a\beta}{\mu} & 0 \\ 0 & -\rho_1 - \rho_2 - \rho_3 - \mu & \frac{a\beta}{\mu} & \frac{a\beta}{\mu} & \frac{a\beta}{\mu} & 0 \\ 0 & \rho_1 & -\mu - \gamma_1 - d_1 & 0 & 0 & 0 \\ 0 & \rho_2 & 0 & -\mu - \gamma_2 - d_2 & 0 & 0 \\ 0 & \rho_3 & 0 & 0 & -\mu - \gamma_3 - d_3 & 0 \\ 0 & 0 & \gamma_1 & \gamma_2 & \gamma_3 & -\mu \end{pmatrix}$$

existing equilibrium point of the model (2) are established.

Let $X^* = (s^*, e^*, i_1^*, i_2^*, i_3^*, r^*, d^*)$ represents any arbitrary equilibrium point (EP) of the model system (2). By solving this equation at the steady state, we have:

$$s^* = \frac{a}{\mu} \left[\frac{1}{(\mathcal{R}_0 - 1) + \beta} \right]$$

$$e^* = \left(\frac{a}{\rho_1 + \rho_2 + \rho_3 + \mu} \right) \left[1 - \frac{1}{\mathcal{R}_0} \right]$$

$$i_2^* = \frac{a\rho_2}{(\rho_2+\rho_2+\rho_3+\mu)(\mu+\gamma_2+d_2)} \left[1 - \frac{1}{\mathcal{R}_0} \right]$$

$$i_3^* = \frac{a\rho_3}{(\rho_1+\rho_2+\rho_3+\mu)(\mu+\gamma_3+d_3)} \left[1 - \frac{1}{\mathcal{R}_0} \right]$$

$$r^* = \frac{a}{\mu(\rho_1+\rho_2+\rho_3+\mu)} \left[1 - \frac{1}{\mathcal{R}_0} \right] \left\{ \frac{\gamma_1\rho_1}{\mu+\gamma_1+d_1} + \frac{\gamma_2\rho_2}{\mu+\gamma_2+d_2} + \frac{\gamma_3\rho_3}{\mu+\gamma_3+d_3} \right\}$$

$$d^* = 1 - (s^* + e^* + i_1^* + i_2^* + i_3^* + r^*)$$

It is clear that the model system (2) has a co-existing equilibrium point (CEP) whenever $\mathcal{R}_0 > 1$ and no positive CEP whenever $\mathcal{R}_0 < 1$. This excludes the possibility of the existence of equilibrium other than disease free equilibrium (DFE) for $\mathcal{R}_0 < 1$.

Moreover, we can show that the DFE X_0^* of the model system (2) is globally asymptotically stable (GAS) whenever $\mathcal{R}_0 < 1$.

Based on the above discussion, the model system (2) has a co-existing equilibrium point, given by X^* , whenever $\mathcal{R}_0 > 1$ and has no CEP for $\mathcal{R}_0 \leq 1$.

Theorem 0.6. *The co-existing equilibrium point X^* is locally asymptotically stable if $\mathcal{R}_0 > 1$*

Proof. Local stability of the co-existing equilibrium point. The Jacobian matrix of the system (2) $J_{X_0^*}$ at DFE is given by:

By using the central manifold theorem [30] to determine the local stability of the co-existing equilibrium, we select β as the bifurcation parameter and gives critical value of β at $\mathcal{R}_0 = 1$ as:

$$\beta^* = \frac{\mu(\rho_1 + \rho_2 + \rho_3 + \mu)(\mu + \gamma_1 + d_1)(\mu + \gamma_2 + d_2)(\mu + \gamma_3 + d_3)}{a \left[\rho_1 (\mu + \gamma_2 + d_2) \tilde{\mathcal{S}} + \rho_2 (\mu + \gamma_1 + d_1) \tilde{\mathcal{S}} + \rho_3 (\mu + \gamma_1 + d_1) (\mu + \gamma_2 + d_2) \right]}$$

where $\tilde{\mathcal{S}} = \mu + \gamma_3 + d_3$

The Jacobian of the system (2) at $\beta = \beta^*$, denoted by $J_{X_0^*}|_{\beta=\beta^*}$ has a right eigenvector (corresponding to the zero eigenvalue) given by $\omega =$

Table 2
Values of the sensitivity indices of \mathcal{R}_0 compared to the parameters system.

Parameters	a	β	ρ_2	ρ_3	ρ_1	γ_1	γ_2	d_3	d_2	d_1	γ_3
Val.	0.304	0.3	0.38	0.048	0.575	0.025	0.0125	0.20	0.0005	0.0001	0.00625
Sens. ind.	1	1	0.169	-0.04	0.034	-0.0146	-0.003	-0.003	-0.0003	-0.00006	-0.0001

$(\omega_1, \omega_2, \omega_3, \omega_4, \omega_5, \omega_6)^T$, where

$$\omega_1 = \frac{-(\rho_1 + \rho_2 + \rho_3 + \mu)}{\mu} \omega_2$$

$$\omega_2 = \omega_2 > 0$$

$$\omega_3 = \left(\frac{\rho_1}{\mu + \gamma_1 + d_1}\right) \omega_2; \omega_4 = \left(\frac{\rho_2}{\mu + \gamma_2 + d_2}\right) \omega_2; \omega_5 = \left(\frac{\rho_3}{\mu + \gamma_3 + d_3}\right) \omega_2$$

$$\omega_6 = \frac{1}{\mu} \left[\frac{\gamma_1 \rho_1}{\mu + \gamma_1 + d_1} + \frac{\gamma_2 \rho_2}{\mu + \gamma_2 + d_2} + \frac{\gamma_3 \rho_3}{\mu + \gamma_3 + d_3} \right] \omega_2$$

Similarly, from $J_{X_0^*}|_{\beta=\beta^*}$, we obtain a left eigenvector $v = (v_1, v_2, v_3, v_4, v_5, v_6)^T$ (corresponding to the zero eigenvalue), where

$$v_1 = 0; v_2 = v_2 > 0; v_3 = \frac{a\beta^*}{\mu(\mu + \gamma_1 + d_1)} v_2; v_4 = \frac{a\beta^*}{\mu(\mu + \gamma_2 + d_2)} v_2; v_5 = \frac{a\beta^*}{\mu(\mu + \gamma_3 + d_3)} v_2; v_6 = 0$$

Using the notations $s = x_1; e = x_2; i_1 = x_3; i_2 = x_4; i_3 = x_5; r = x_6$ et $d = x_7$

Hence, we have

$$\tilde{a} = \sum_{k,i,j=1}^7 v_k \omega_i \omega_j \frac{\partial^2 f_k(0,0)}{\partial x_i \partial x_j} \text{ and } \tilde{b} = \sum_{k,i=1}^7 v_k \omega_i \frac{\partial^2 f_k(0,0)}{\partial x_i \partial \beta}$$

By replacing values of all the second-order derivatives measured at disease free equilibrium and $\beta = \beta^*$ we obtain:

$$\begin{aligned} f_1 &= a - \beta x_1 x_3 - \beta x_1 x_4 - \beta x_1 x_5 - \mu x_1 \\ f_2 &= \beta x_1 x_3 + \beta x_1 x_4 + \beta x_1 x_5 - (\rho_1 + \rho_2 + \rho_3 + \mu) x_2 \\ f_3 &= \rho_1 x_2 - (\mu + \gamma_1 + d_1) x_3 \\ f_4 &= \rho_2 x_2 - (\mu + \gamma_2 + d_2) x_4 \\ f_5 &= \rho_3 x_2 - (\mu + \gamma_3 + d_3) x_5 \\ f_6 &= \gamma_1 x_3 - \gamma_2 x_4 + \gamma_3 x_5 - \mu x_6 \\ f_7 &= d_1 x_3 - d_2 x_4 + d_3 x_5 \\ \tilde{a} &= (v_1 \omega_1 \omega_3 + v_1 \omega_1 \omega_4 + v_1 \omega_1 \omega_5)(-\beta) + (v_2 \omega_1 \omega_3 + v_2 \omega_1 \omega_4 + v_2 \omega_1 \omega_5)(-\beta) \\ \tilde{b} &= v_1 \omega_1 (-x_3 - x_4 - x_5)|_{(0,0)} + v_1 \omega_3 (-x_1)|_{(0,0)} + v_1 \omega_4 (-x_1)|_{(0,0)} + v_1 \omega_5 (-x_1)|_{(0,0)} \\ \tilde{a} &= (v_2 \omega_1 \omega_3 + v_2 \omega_1 \omega_4 + v_2 \omega_1 \omega_5)(\beta^*) \\ \tilde{b} &= v_2 \omega_1 (x_3 + x_4 + x_5)|_{(x_0^*,0)} + x_1 (v_2 \omega_3 + v_2 \omega_4 + v_2 \omega_5)|_{(x_0^*,0)} \end{aligned}$$

$$\tilde{a} = \frac{-v_2}{a} [(\rho_1 + \rho_2 + \rho_3 + \mu) \omega_2]^2 < 0$$

and

$$\tilde{b} = \frac{a}{\mu} v_2 \left(\frac{\rho_1}{\mu + \omega_1 + d_1} + \frac{\rho_2}{\mu + \omega_2 + d_2} + \frac{\rho_3}{\mu + \omega_3 + d_3} \right) \omega^2 > 0$$

As $\tilde{a} < 0$ and $\tilde{b} > 0$ at $\beta = \beta^*$, thus applying the Remark 1 of the Theorem 4.1 presented in [30], a transcritical bifurcation occurs at $\mathcal{R}_0 = 1$.

Remark 0.7. The stability of DFE means that solutions with initial values close to X_0^* remain close to the equilibrium and approach the equilibrium as $t \rightarrow \infty$. Local stability of an equilibrium point means that if you put the system somewhere nearby the point then it will move itself to the equilibrium point in some time. Global stability means that the

system will come to the equilibrium point from any possible starting point (i.e, there is no "nearby" condition). If the quantity \mathcal{R}_0 , that is the average number of the secondary infections produced by one infected individual during the entire course of infection in a completely susceptible population, is greater than one, the epidemiological interpretation indicates that COVID-19 may keep persistent in the population, that is the disease-free equilibrium is unstable and there is a co-existing equilibrium point, given by X^* , that is (locally) asymptotically stable. **Theorem 0.6** confirms the persistence of the disease when $\mathcal{R}_0 > 1$.

Elasticity of the basic reproduction number \mathcal{R}_0 with respect to the model parameters

Let \mathcal{K} be a variable that depends on parameters $\varpi_1, \varpi_2, \varpi_3, \dots, \varpi_n$, the sensitivity index $\mathcal{S}_{\varpi_i}^{\mathcal{K}}$ of the variable \mathcal{K} with respect to the parameter ϖ_i is given by:

$$\mathcal{S}_{\varpi_i}^{\mathcal{K}} = \frac{\partial \mathcal{K}}{\partial \varpi_i} \frac{\varpi_i}{\mathcal{K}} \tag{5}$$

The sensitivity index measures the relative change in a state variable \mathcal{K} , which results from a relative change in the parameter ϖ_i . Given the explicit formula of the basic reproduction number (\mathcal{R}_0), we derive the analytical expressions to obtain the sensitivity of this \mathcal{R}_0 . Values of the sensitivity indices of \mathcal{R}_0 (eq. (3)) compared to the parameters system (Table 1) are presented in Table 2.

The basic reproduction number is more sensitive to the parameter with the highest elasticity index value (a, β and ρ_2) and the least sensitive to the parameter with the lowest elasticity index value (other parameter).

Optimal Control

Description and settings

In this section, we discuss some control's techniques that consist in limiting contact between infected and susceptible individuals, as well as the screening and treatment of individuals infected with COVID-19. Because of the costs due to the application of these measures, the problem is presented as that of minimizing this cost during the whole time that these measures are applied. We use Pontryagin's Maximum Principle [16,31] to determine the explicit analytical expression of this control. Considering model (1), we define the following control measures:

1. The control noted ξ_1 , modeling all efforts to prevent the transmission of infection between individuals in the population. It takes into account the different strategies used to reduce the number of contacts between susceptible and infected individuals. These include efforts to isolate, quarantine patients under treatment, the wearing of masks and any strategy to avoid further contamination due to direct contact. The action of this control is limited in the range $[0; T]$.
2. The control ξ_2 modeling all treatment efforts for individuals who are COVID-19 positive in the range $[0; T]$.

Control functions $\xi_1(t)$ and $\xi_2(t)$ are bounded, Lebesgue integrable functions defined in $[0, 1]$. If the value of the control function ξ_1 is close to the value 1, in this case the contacts between susceptible and infected are low and in this case there are very few cases of transmission of the

disease. If the value of the control function ξ_2 is close to the value 1, in this case the efforts to treat the infected are at their maximum. We will consider the case where the value of the baseline reproduction rate $R_0 > 1$, so we are not in the stability zone of DFE and that is necessary to apply the control measures in order to limit the transmission of COVID-19. Based on conditions depicted above, the optimal control problem can be formulated as follows:

$$\begin{cases} \dot{s} = a - \beta(1 - \xi_1)(i_1 + i_2 + i_3)s - \mu s \\ \dot{e} = \beta(1 - \xi_1)(i_1 + i_2 + i_3)s - (\mu + \rho_1 + \rho_2 + \rho_3)e \\ \dot{i}_1 = \rho_1 e - (\mu + \gamma_1 + \gamma_1^* \xi_2 + d_1)e_1 \\ \dot{i}_2 = \rho_2 e - (\mu + \gamma_2 + \gamma_2^* \xi_2 + d_2)e_2 \\ \dot{i}_3 = \rho_3 e - (\mu + \gamma_3 + \gamma_3^* \xi_2 + d_3)e_3 \\ \dot{r} = \gamma_1 i_1 + \gamma_2 i_2 + \gamma_3 i_3 - \mu r \\ \dot{d} = d_1 e_1 + d_2 e_2 + d_3 e_3 \end{cases} \quad (6)$$

where $\gamma_1^*, \gamma_2^*, \gamma_3^*$ are per-capita treatment rates for infectious individuals from group 1, 2 and 3 respectively and then $(\gamma_i + \gamma_i^* \xi_2)$ give the proportion of individuals recovery for $i = 1, 2, 3$. On the other hand, if $\xi_1 = 1$, then the number of infectious-susceptible contacts is zero and if $\xi_1 = 0$, the infection rate is maximum and equal to β . If $\xi_2 = 1$, then $\gamma_i^*, i = 1, 2, 3$ gives the proportion of actual treatment for infected of i group and $\gamma_i^* \xi_2$ gives the proportion of humans cured with treatment for $i = 1, 2, 3$. If $\xi_2 = 0$, it's the case where there is no treatment.

Theorem 0.8. $\Omega \times \Gamma = [0, 1]$ is positively invariant for the system Eq. (6).

Proof. Considering the Gronwall inequality, given that all the variables of this system are positive, we have:

$$\begin{aligned} \frac{ds}{dt} &\leq a - \beta(i_2 + i_2 + i_3)s - \mu s \\ \frac{de}{dt} &\leq \beta(i_2 + i_2 + i_3)s - (\mu + \rho_1 + \rho_2 + \rho_3)e \\ \frac{di_1}{dt} &\leq \rho_1 e - (\mu + \gamma_1 + d_1)e_1 \\ \frac{di_2}{dt} &\leq \rho_2 e - (\mu + \gamma_2 + d_1)e_2 \\ \frac{di_3}{dt} &\leq \rho_3 e - (\mu + \gamma_3 + d_1)e_3 \\ \dot{r} &\leq \gamma_1 i_1 + \gamma_2 i_2 + \gamma_3 i_3 \\ \dot{d} &\leq \gamma_1 i_1 + \gamma_2 i_2 + \gamma_3 i_3 \end{aligned}$$

Note that the right-hand side member of this inequation system represents model (1) of the COVID-19 transmission without control. Knowing that the solution of this system (1) is defined in Ω . Thus, applying the Gronwall inequality, we deduce that the solutions of the model system (6) are bounded as $\xi_i \in [0, 1] \forall i \in \{1, 2\}$.

To the system (2) associate the fonction J shown in (7) to obtain the optimal control problem.

$$J(\xi_1, \xi_2) = \int_0^T \left[A_1 i_1 + A_2 i_2 + A_3 i_3 + \frac{B_1 \xi_1^2}{2} + \frac{B_2 \xi_2^2}{2} \right] dt \quad (7)$$

Where A_1, A_2 and A_3 represent the costs of taking care of infectious individual type i_1, i_2 and i_3 respectively. The constants B_1 is positive and correspond to the effort used to regulate the contact between individuals in the population and B_2 is positive and correspond to the effort used to treat infectious individuals in the population.

As given in the litterature, the cost function is assured to be a quadratic function is a natural way that allows the analogy with the expended energy for all those dimesions. The objective is to limit the spread of the disease by reducing the number of contact between in-

fectious and susceptible individuals, and treating infectious cases. We then look of the control terms ξ_1 and ξ_2 that minimize the cost:

$$J^*(\xi_1, \xi_2) = \min \left\{ J(\xi_1, \xi_2) \Big|_{\xi_i \in \Gamma} \right\} \text{ where } \Gamma = \left\{ \xi_i^*, \tilde{a} < \xi_i^* < \tilde{b} \right\} \text{ for } i = 1, 2$$

with ξ_i a piecewise continuous function on $[0, T]$.

The aim is not only to reduce infected individuals after a times T but also over $[0, T]$ to act simultaneously on prevention (contact infectious - susceptible individuals). The first term of the functional J models the proportion of infected individuals accumulated from the initial time $\tau_0 = 0$ to the final time $\tau_f = T$. The choice of the positive parameters A_1, A_2, A_3, B_1 and B_2 depends on the relative, subjective importance that the members of the technical staff give to reduce the number of individuals infected by applying treatment, limiting the number of contacts between infected and susceptible individuals according to age group. Γ is the set of controls ξ_1 and ξ_2 , and a_1 and b_1 are constants in the interval $[0, 1]$.

The optimal control problem is completely solved when the analytical expressions of ξ_1^* and ξ_2^* witch belong to Γ that minimize the functional J given in (7) are determined.

Existence of the optimal control

In this subsection, we show the existence of an optimal control.

Theorem 0.9. Consider the control problem associated with problems (6)–(7). There is a control (ξ_1^*, ξ_2^*) and a corresponding solution $(s^*, e^*, i_1^*, i_2^*, i_3^*)$ which minimizes $J(\xi_1^*, \xi_2^*)$ on Γ such that

$$\min_{(\xi_1, \xi_2) \in \Gamma} J(\xi_1, \xi_2) = J(\xi_1^*, \xi_2^*)$$

Proof. Considering [31], we should verify that the following requirements are met:

1. The set of controls corresponding to the solutions of this problem is not empty;
2. The set of controls Γ is related and closed in $L^2[0, T]$;
3. The set of solutions of the state system is bounded by a linear control function;
4. The integrand of the objective function (cout) is convex;
5. The existence of non-negative constants c_1, c_2 and γ such that the integrand of the objective function is bounded by:

$$c_1 \left(|\xi_1|^2 + |\xi_2|^2 \right)^{\gamma-1} - c_2$$

We can also chech that $\xi_1 = \xi_2 = 0$ is a control in Γ and $(s^*, e^*, i_1^*, i_2^*, i_3^*)$ is a solution corresponding to control $\xi_1 = \xi_2 = 0$, so the set of all controls and corresponding solutions is not empty, which satisfies condition 1. By definition, the range of controls is limited, which satisfies condition 2. The right-hand member of the state system (6) satisfies condition 3 because the solutions of this system are bounded. The integrand of functional J is clearly convex in the Γ , showing that condition 4 is satisfied. Finally, there are $c_1, c_2 > 0$ and $\gamma > 1$ satisfying

$$A_1 i_1(t) + A_2 i_2(t) + A_3 i_3(t) + \frac{B_1 \xi_1^2}{2} + \frac{B_2 \xi_2^2}{2} \geq c_1 \left(|\xi_1|^2 + |\xi_2|^2 \right)^{\gamma-1} - c_2,$$

because the states variables are bounded. We conclude that there exists an optimal control (ξ_1^*, ξ_2^*) that minimizing the objective functional $J(\xi_1, \xi_2)$. The boundary and the fact that the boundaries are finite ensure the compactness required for optimal control. The considered initial conditions are $i_1(0), i_2(0)$ and $i_3(0)$. \square At present we have ensured the existence of an optimal control. To solve this problem, we can use the

maximum Pontryagin principle.

Characterization of optimal central

In this subsection, we give its characterization.

Theorem 0.10. *The optimal control which minimizes the functional J given in (7) under the constraints given by the system of differential Eqs. (6) is given by:*

$$\xi_1^* = \max \left\{ a_1, \min \left\{ b_1, \frac{1}{B_1} [(\lambda_2 - \lambda_1)(i_1 + i_2 + i_3)\beta s] \right\} \right\}$$

$$\xi_2^* = \max \left\{ a_2, \min \left\{ b_2, \frac{1}{B_2} [(\lambda_3\gamma_1^*i_1 + \lambda_4\gamma_2^*i_2 + i_2 + \lambda_5\gamma_3^*i_3)] \right\} \right\}$$

Proof. Let $Z = (s, e, i_1, i_2, i_3, r, d) \in \Omega, U = (\xi_1, \xi_2) \in \Gamma$ and $\mathcal{F} = (\lambda_1, \lambda_2, \lambda_3, \dots, \lambda_7)$ be the adjoint variables. We define the Lagrangian (Hamiltonian and penalties) associated with the problem defined above:

$$\begin{aligned} \mathcal{L}(Z, U, \mathcal{F}) = & A_1i_1 + A_2i_2 + A_3i_3 + \frac{1}{2}B_1\xi_1^2 + \frac{1}{2}B_2\xi_2^2 \\ & + \lambda_1 \left[a - \beta(1 - \xi_1)(i_1 + i_2 + i_3)s - \mu s \right] \\ & + \lambda_2 \left[\beta(1 - \xi_1)(i_1 + i_2 + i_3)s - (\mu + \rho_1 + \rho_2 + \rho_3)e \right] \\ & + \lambda_3 \left[\rho_1e - (\mu + \gamma_1 + \gamma_1^*\xi_2 + d_1)i_1 \right] \\ & + \lambda_4 \left[\rho_2e - (\mu + \gamma_2 + \gamma_2^*\xi_2 + d_2)i_2 \right] \\ & + \lambda_5 \left[\rho_3e - (\mu + \gamma_3 + \gamma_3^*\xi_2 + d_3)i_3 \right] \\ & + \lambda_6 \left[\gamma_1i_1 + \gamma_2i_2 + \gamma_3i_3 - \mu r \right] + \lambda_7 \left[d_1i_1 + d_2i_2 + d_3i_3 \right] \\ & + \omega_1(\xi_1 - a_1) + \omega_2(b_1 - \xi_1) + \omega_3(\xi_2 - a_2) + \omega_4(b_2 - \xi_2) \end{aligned}$$

where $\omega_1, \omega_2, \omega_3$ and ω_4 are penalty variables attached to control ξ_1 and ξ_2 . These penalty multipliers must meet the following conditions:

$$\omega_1(\xi_1 - a_1) = 0; \omega_2(b_1 - \xi_1) = 0; \omega_3(\xi_2 - a_2) = 0; \omega_4(b_2 - \xi_2) = 0$$

In addition, the differential equations which govern the adjoint variables are obtained by differentiating the Lagrangian (as per Maximum Principle)

$$\begin{aligned} \frac{d\lambda_1}{dt} = -\frac{\partial \mathcal{L}}{\partial s}; \frac{d\lambda_2}{dt} = -\frac{\partial \mathcal{L}}{\partial e}; \frac{d\lambda_3}{dt} = -\frac{\partial \mathcal{L}}{\partial i_1}; \frac{d\lambda_4}{dt} = -\frac{\partial \mathcal{L}}{\partial i_2}; \frac{d\lambda_5}{dt} = -\frac{\partial \mathcal{L}}{\partial i_3}; \\ = -\frac{\partial \mathcal{L}}{\partial i_3}; \frac{d\lambda_6}{dt} = -\frac{\partial \mathcal{L}}{\partial r}; \frac{d\lambda_7}{dt} = -\frac{\partial \mathcal{L}}{\partial d} \end{aligned}$$

That gives the adjoint system below:

$$\begin{cases} \frac{d\lambda_1}{dt} = \beta(1 - \xi_1)(i_1 + i_2 + i_3) + \mu - \lambda_2\beta(1 - \xi_1)(i_1 + i_2 + i_3), \\ \frac{d\lambda_2}{dt} = \lambda_2(\mu + \rho_1 + \rho_2 + \rho_3) - \lambda_3\rho_1 - \lambda_4\rho_2 - \lambda_5\rho_3, \\ \frac{d\lambda_3}{dt} = A_1 + \lambda_1\beta(1 - \xi_1)s - \lambda_2\beta(1 - \xi_1)s + \lambda_3(\mu + \gamma_1 + \gamma_1^*\xi_2 + d_1) - \lambda_6\gamma_1 - \lambda_7d_1, \\ \frac{d\lambda_4}{dt} = A_2 + \lambda_1\beta(1 - \xi_1)s - \lambda_2\beta(1 - \xi_1)s + \lambda_4(\mu + \gamma_2 + \gamma_2^*\xi_2 + d_2) - \lambda_6\gamma_2 - \lambda_7d_2, \\ \frac{d\lambda_5}{dt} = A_3 + \lambda_1\beta(1 - \xi_1)s - \lambda_2\beta(1 - \xi_1)s + \lambda_5(\mu + \gamma_3 + \gamma_3^*\xi_2 + d_3) - \lambda_6\gamma_3 - \lambda_7d_3, \\ \frac{d\lambda_6}{dt} = \lambda_6\mu, \\ \frac{d\lambda_7}{dt} = 0. \end{cases}$$

For these adjoint variables, we must have $\lambda_i(T) = 0, i = 1, \dots, 7$, there are the transversality conditions also called marriage conditions.

The value of the optimal control can be characterized at each instant $t \in [0, T]$ by noting that it minimizes the Lagrangian (Pontryagin's Maximum Principle) and that's at this optimal control, variables must satisfy the necessary condition:

$$\frac{\partial \mathcal{L}}{\partial \phi^*} = 0 \text{ with } \phi^* = (\xi_1^*, \xi_2^*) \text{ the optimal couple}$$

Given that:

$$\begin{aligned} \mathcal{L} = & \frac{1}{2}B_1\xi_1^2 + \frac{1}{2}B_2\xi_2^2 + \lambda_1 \left[a - \beta(1 - \xi_1)(i_1 + i_2 + i_3)s - \mu s \right] \\ & + \lambda_2 \left[\beta(1 - \xi_1)(i_1 + i_2 + i_3)s - (\mu + \rho_1 + \rho_2 + \rho_3)e \right] \\ & + \lambda_3 \left[\rho_1e - (\mu + \gamma_1 + \gamma_1^*\xi_2 + d_1)i_1 \right] + \lambda_4 \left[\rho_2e - (\mu + \gamma_2 + \gamma_2^*\xi_2 + d_2)i_2 \right] \\ & + \lambda_5 \left[\rho_3e - (\mu + \gamma_3 + \gamma_3^*\xi_2 + d_3)i_3 \right] + \omega_1(\xi_1 - a_1) + \omega_2(b_1 - \xi_1) \\ & + \omega_3(\xi_2 - a_2) + \omega_4(b_2 - \xi_2) + (\text{terms without } \xi_1 \text{ nor } \xi_2) \end{aligned}$$

Differentiating \mathcal{L} with respect to ξ_1 and ξ_2 gives respectively:

$$\frac{\partial \mathcal{L}}{\partial \xi_1} = B_1\xi_1 + \lambda_1\beta(i_1 + i_2 + i_3)s - \beta\lambda_2(i_1 + i_2 + i_3)s + \omega_1 - \omega_2$$

$$\frac{\partial \mathcal{L}}{\partial \xi_2} = B_2\xi_2 + \lambda_3\omega_1^*i_1 - \lambda_4\omega_2^*i_2 - \lambda_5\omega_3^*i_3 + \omega_3 - \omega_4$$

At (ξ_1^*, ξ_2^*) , we have $\frac{\partial \mathcal{L}}{\partial \xi_1} = \frac{\partial \mathcal{L}}{\partial \xi_2} = 0$ the equalities give:

$$\begin{cases} \frac{\partial \mathcal{L}}{\partial \xi_1} = B_1\xi_1 + \lambda_1\beta(i_1 + i_2 + i_3)s - \beta\lambda_2(i_1 + i_2 + i_3)s + \omega_1 - \omega_2 = 0 \\ \frac{\partial \mathcal{L}}{\partial \xi_2} = B_2\xi_2 + \lambda_3\omega_1^*i_1 - \lambda_4\omega_2^*i_2 - \lambda_5\omega_3^*i_3 + \omega_3 - \omega_4 = 0 \end{cases}$$

Hence, we get the optimum

$$\begin{cases} \xi_1^* = \frac{1}{B_1} [\beta(i_1 + i_2 + i_3) [\lambda_2 - \lambda_1] s + \omega_2 - \omega_1] \\ \xi_2^* = \frac{1}{B_2} [\lambda_3 \gamma_1^* i_1 + \lambda_4 \gamma_2^* i_2 + \lambda_5 \gamma_3^* i_3 + \omega_4 - \omega_3] \end{cases}$$

For a more explicit formula for optimal controls without $\omega_1, \omega_2, \omega_3$ and ω_4 , we use standard techniques.

For this purpose, we consider 6 cases, with 3 cases for each optimal control:

- Case 1: In the set $\{t, a_1 < \xi_1^* < b_1\}, \omega_1(\xi_1^* - a_1) = \omega_2(b_1 - \xi_1^*) = 0 \Rightarrow \omega_1 = \omega_2 = 0$. So the optimal control is:

$$\xi_1^* = \frac{1}{B_1} \left[(\lambda_2 - \lambda_1) \beta (i_1 + i_2 + i_3) s \right]$$

- Case 2: In the set $\{t, \xi_1^* = b_1\}, \xi_1^* = \frac{1}{B_1} [\beta(\lambda_2 - \lambda_1) (i_1 + i_2 + i_3) s + \omega] = b_1$

$$b_1 = \xi_1^* = \frac{1}{B_1} \left[(\lambda_2 - \lambda_1) \beta (i_1 + i_2 + i_3) s \right] \leq b_1 \text{ with } \omega_2(t) \geq 0$$

- Case 3: In the set $\{t, \xi_1^* = a_1\}, \omega_1(\xi_1^* - a_1) = \omega_2(b_1 - \xi_1^*) = 0 \Rightarrow \omega = 0$ from where

$$a_1 = \xi_1^* = \frac{1}{B_1} \left[(\lambda_2 - \lambda_1) \beta (i_1 + i_2 + i_3) s - \omega_1 \right]$$

and therefore

$$\xi_1^* = \frac{1}{B_1} \left[(\lambda_2 - \lambda_1) \beta (i_1 + i_2 + i_3) s \right] \geq a_1 \text{ with } \omega_3(t) \geq 0$$

- Case 4: In the set $\{t, a_1 < \xi_2^* < b_1\}, \omega_3(\xi_2^* - a_2) = \omega_4(b_2 - \xi_2^*) = 0 \Rightarrow \omega_3 = \omega_4 = 0$ So the optimal control is

$$\xi_2^* = \frac{1}{B_2} [\lambda_3 \gamma_1^* i_1 + \lambda_4 \gamma_2^* i_2 + \lambda_5 \gamma_3^* i_3]$$

- Case 5: In the set $\{t, \xi_2^* = b_2\}, \xi_2^*(\xi_2^* - a_2) = \omega_4(b_2 - \xi_2^*) = 0 \Rightarrow \omega_3 = 0$, hence

$$b_2 = \xi_2^* = \frac{1}{B_2} [\lambda_3 \omega_1^* i_1 + \lambda_4 \omega_2^* i_2 + \lambda_5 \omega_3^* i_3 + \omega_4]$$

As $\omega \geq 0$, so the optimal control is

$$\xi_2^* = \frac{1}{B_2} [\lambda_3 \omega_1^* i_1 + \lambda_4 \omega_2^* i_2 + \lambda_5 \omega_3^* i_3] \leq b_2$$

- Case 6 In the set $\{t, \xi_2^* = a_2\}, \omega_3(\xi_2^* - a_2) = \omega_4(b_2 - \xi_2^*) = 0 \Rightarrow \omega_4 = 0$, hence $a_2 = \xi_2^* = \frac{1}{B_2} [\lambda_3 \omega_1^* i_1 + \lambda_4 \omega_2^* i_2 + \lambda_5 \omega_3^* i_3 - \omega_3]$ As $\omega \geq 0$, so the

optimal control is $\xi_2^* = \frac{1}{B_2} [\lambda_3 \gamma_1^* i_1 + \lambda_4 \omega_2^* i_2 + \lambda_5 \gamma_3^* i_3] \geq a_2$ with these

cases, we rewrite the expression of the first and second controls:

$$\xi_1^* = \max \left\{ a_1, \min \left\{ b_1, \frac{s}{B_1} [(\lambda_2 - \lambda_1) \beta (i_1 + i_2 + i_3)] \right\} \right\}$$

$$\xi_2^* = \max \left\{ a_1, \min \left\{ b_2, \frac{s}{B_2} [\lambda_3 \gamma_1^* i_1 + \lambda_4 \gamma_2^* i_2 + \lambda_5 \gamma_3^* i_3] \right\} \right\}$$

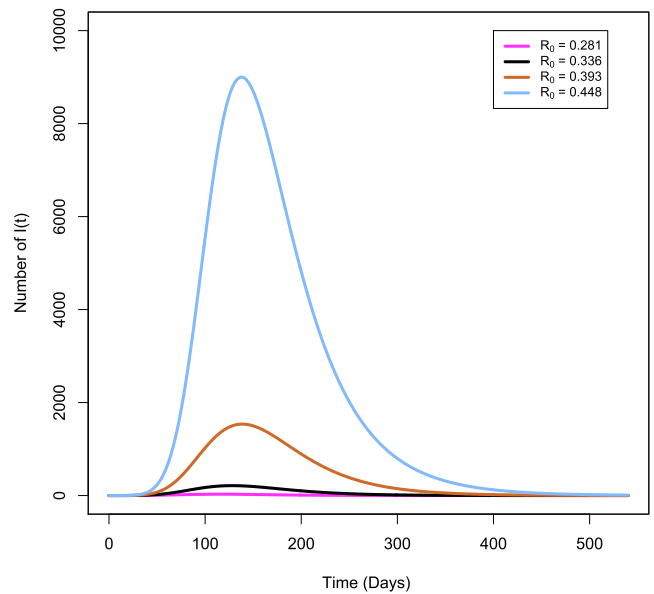


Fig. 2. Evolution of infected individuals $I(t)$ for several values of \mathcal{R}_0 ($\mathcal{R}_0 < 1$) with different values of β in (0.10, 0.22, 0.32, 0.43).

This completes the proof of the theorem.

Numerical simulations

In this section we present simulations that have been carried out. Some curves of the dynamics of the disease according to different values of the basic reproduction number are displayed. The first group of plots shows the situation of $\mathcal{R}_0 < 1$ and the second presents the situation of $\mathcal{R}_0 > 1$ with and without control. Others plots are devoted to the dynamics of the global stability of DFE and the co-existing equilibrium for different plans.

Fig. 2 shows that with $\mathcal{R}_0 < 1$, the disease is eliminated in the Congolese population. Figs. 3(a) and 3(b) show the evolution of infected individuals when $\mathcal{R}_0 > 1$ without any control measures. Here results show that there is a co-existing equilibrium point (CEP), this means that the disease will persist in the population if control measures are not applied.

Figs. 4–7 show that the application of control measures on the pandemic have an impact on the evolution of the disease towards a possible extinction in the future.

Now we present the graphs showing the global stability of the equilibrium points of DFE and the co-existing equilibrium respectively in Figs. 8 and 9. With baseline parameter values presented in Table 1 and considering that recruitment is defined by $a^* = aN$, with N the total population, the coordinate of X_0^* is given by: $X_0^* = (416666.67, 0, 0, 0, 0, 0)$.

The co-existing equilibrium is defined by $X^* = (s^*, e^*, i_1^*, i_2^*, i_3^*, r^*, d^*)$, with baseline parameter values presented in Table 1 is given by:

$$X^* = (0.46, 7849.28, 48725.81, 165029.99, 1671.17, 178076.59, 401352.32).$$

Discussion of results and conclusion

General discussion

The baseline situation reflects the evolution of the pandemic at the beginning of its installation, without optimal control. The progression is rapid due to the transmission, initially less pronounced with a daily increase until it reaches its peak. We note that, the co-existing equilibrium point for the infectious compartment is stable as shown in Figs. 2

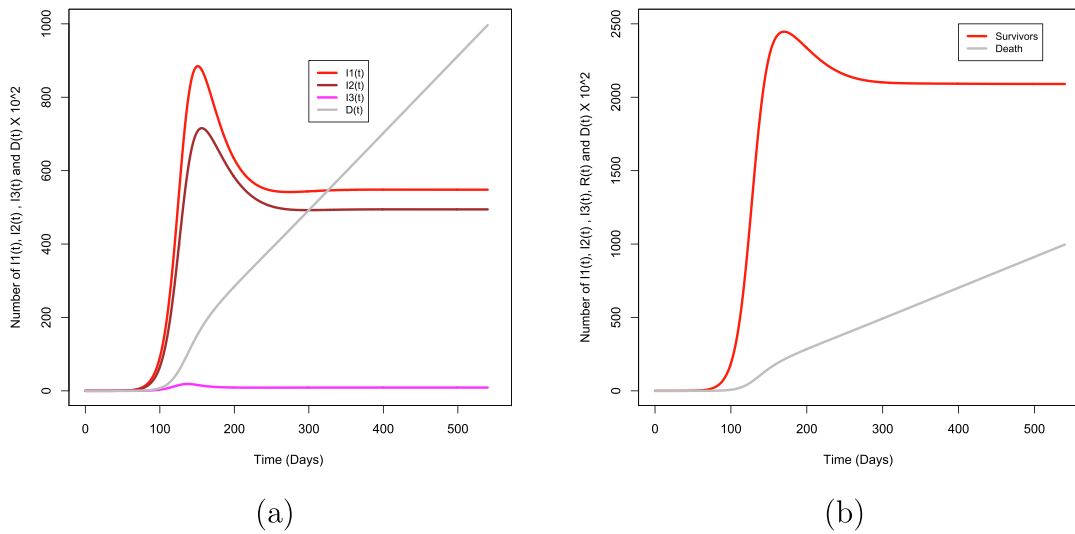


Fig. 3. Evolution infectious individuals and deaths, initial values $S_0 = 80.10^6$ and $I_1(0) = I_2(0) = I_3(0) = 1$ with baseline parameter values given in Table 1 and $\mathcal{R}_0 = 3.054$. In (a) the evolution of I_1, I_2, I_3 and D is presented, in (b) the evolution of $I = I_1 + I_2 + I_3 + R$ and D is presented.

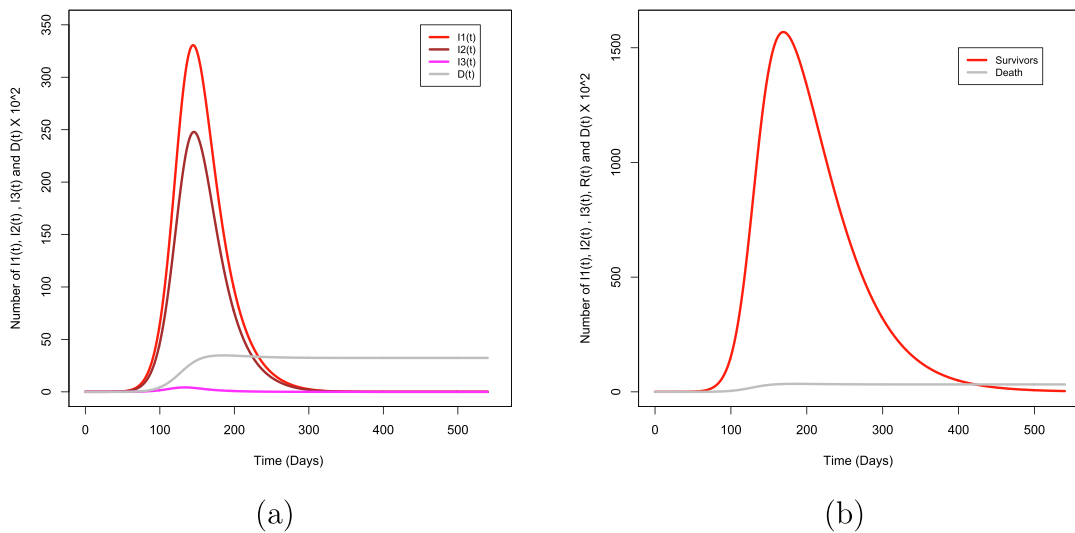


Fig. 4. Shows the evolution of the system when control measures are applied into the situation presented in Figs. 3(a) and 3(b).

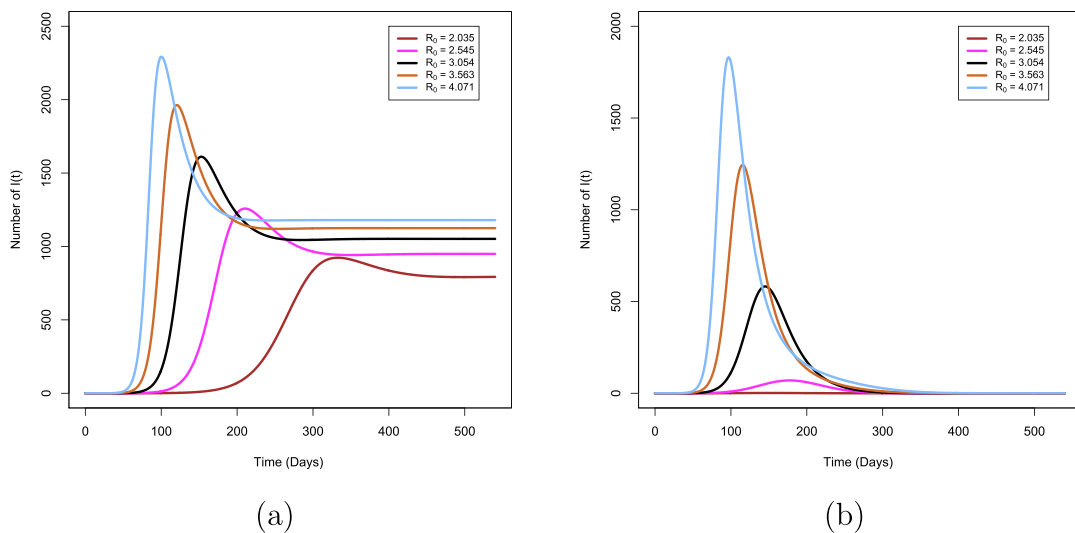


Fig. 5. Evolution of $I(t)$ for several values of \mathcal{R}_0 and use of basic parameters (Table 1) (a) without control (b) with control by applying the protocol of decreasing the dead rate due to COVID-19 and increasing the recovered rate.

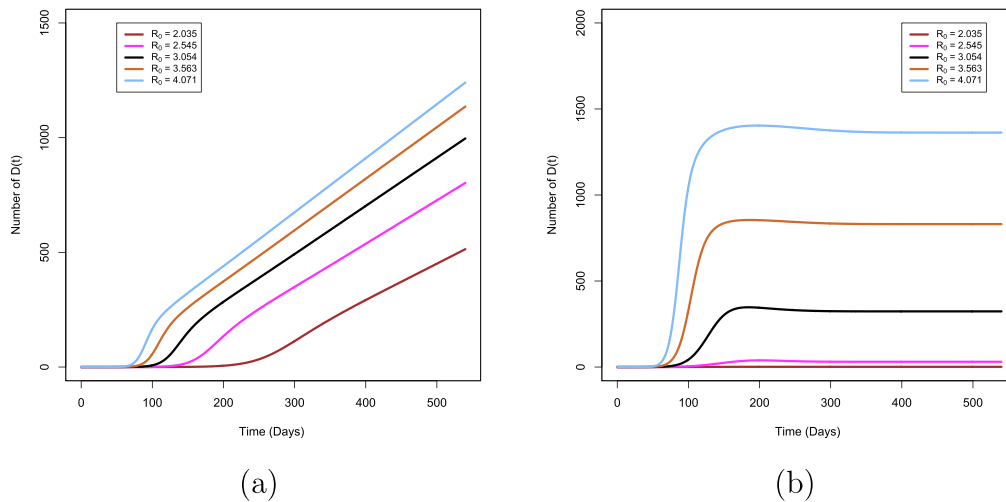


Fig. 6. Evolution of $D(t)$ for several values of R_0 and use of basic parameter (Table 1) (a) without control (b) with control by applying the protocol of decreasing the dead rate due to COVID-19 and increasing the recovered rate.

and 3. The numerical simulation carried out on a initial population of susceptible $S_0 = 80 \times 10^6$ we obtain a maximum incidence of $161139[14 \times 10^4, 18 \times 10^4]$ cases. The total number of patients that can be registered calculated is estimated at 6419 cases at the 3rd month, 13906 cases at the 6th month and 10511 cases at the 12th month. The calculated R_0 is 3.054.

To control the pandemic, a protocol is applied from the end of the second month (60 days) since the beginning of the disease in DRC. The effect of this control is to reduce, at each time step (day), the death rates $d_i (i = 1, 2, 3)$ of the assumed values 0.000009 for the forms I_1 and I_2 , and 0.0001 for the form I_3 , representing a management effort for all categories of people with a special focus on individuals of type I_3 . At the same time, an increase from the assumed values 0.00050, 0.00050 and 0.0050 to the recovered rates $\gamma_i (i = 1, 2, 3)$, respectively for the type I_1 , I_2 , and I_3 , representing the action of reduction in transmission, improved screening, treatment for individuals diagnosed positive to COVID-19 and the implementation of barrier measures limiting contamination for undiagnosed individuals. The results of these control measures show that a co-existing disease-free equilibrium will be observed after 1.5 years since the beginning of the pandemic. Fig. 4 illustrate this control with in (a) individuals I_1, I_2 and I_3 are shown separately and in (b)

surviving individuals are represented by the sum of I_1, I_2, I_3 and R . Note that the optimal control here is represented in an empirically imputed incremental change. Taking the control measures into account, we have a decrease in the basic reproduction number which leads to a disease-free equilibrium earlier with a reduction in the number of deaths. As shown in Fig. 6, if control measures are not taken into account, the number of dead individuals due to COVID-19 $D(t)$ increases exponentially, but when control is applied, stability of $D(t)$ is observed later. Based on the results obtained in Figs. 7, if control measures are not taken into account, the number of recovered individuals remains high due to the large number of infected individuals, whereas if control measures are taken into account, $R(t)$ individuals drop to the disease-free equilibrium.

Based on the results presented in Figs. 8 and 9, it appears that the policy of the DRC response team is more focused on reducing the number of deaths and stabilisation of infected individuals. We find that in DRC younger individuals are the most infected with COVID-19 and older (old) individuals die more from COVID-19 infection compared to other categories, this is justified by the fact that the elderly often have co-morbidities and the young do not fully comply with the barrier measures as requested by the government.

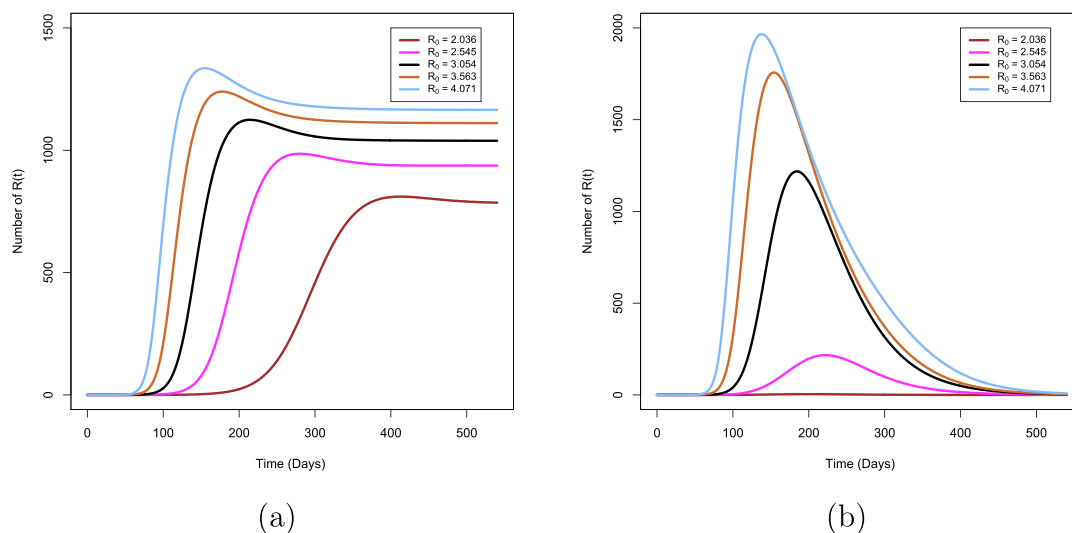


Fig. 7. Evolution of $R(t)$ for several values of R_0 and use of basic parameter (Table 1) (a) without control (b) with control by applying the protocol of decreasing the dead rate due to COVID-19 and increasing the recovered rate.

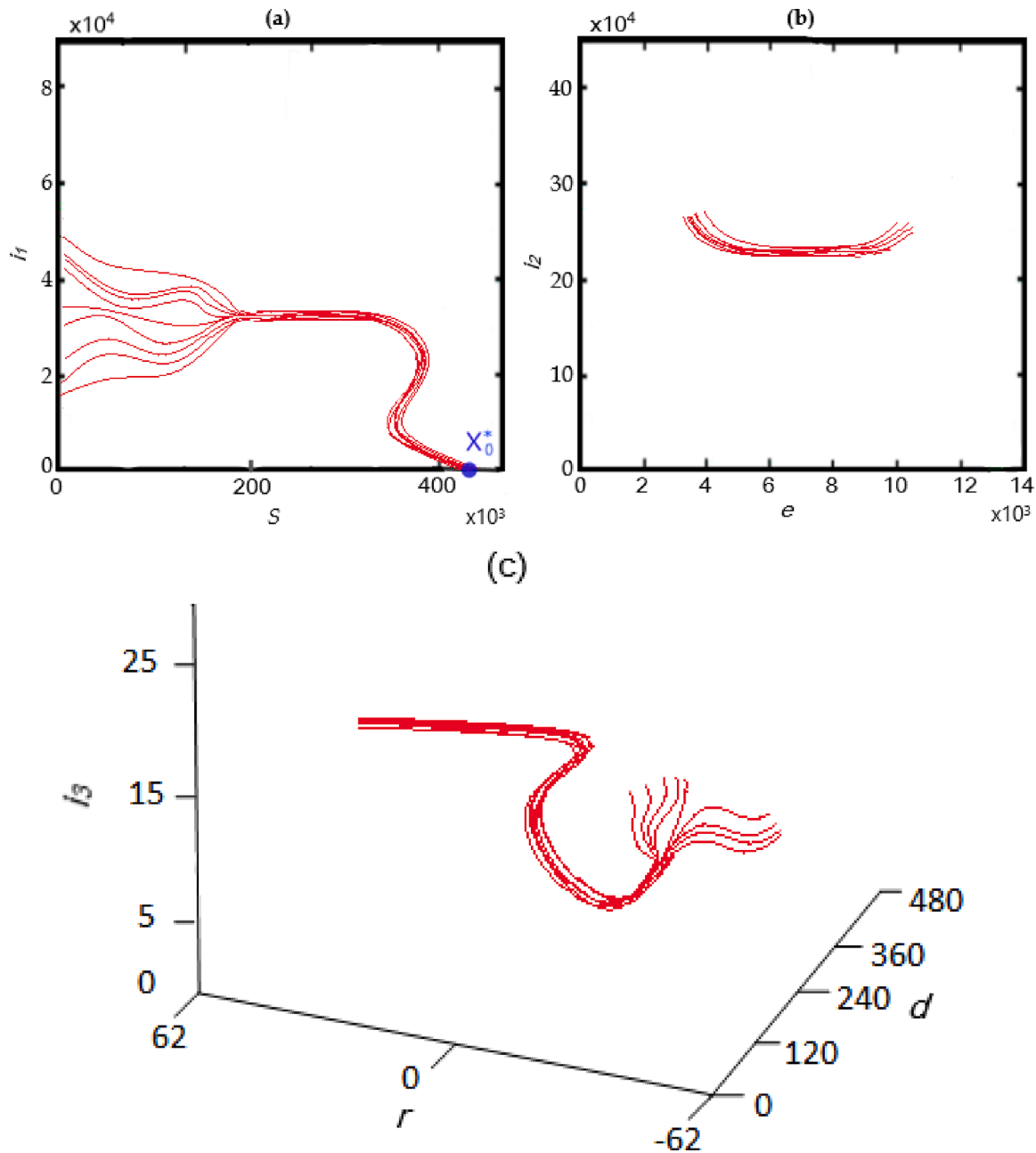


Fig. 8. (a), (b) and (c) display the dynamics of the global stability of DFE, noted by X^* respectively different plans (I_1, s) , (I_2, e) and (I_3, r, d) .

In DRC, the various reports of the response team give us the number of new cases reported on the basis of the tests carried out and to date less than 500/ day. Knowing that the health coverage and the screening capacity for the detection of COVID-19 in DRC is estimated at less than 20%, in addition to these are people escaping the official health care system (recourse to traditional medicine and in private structures, or at home with self-medication, ...), it is clear that the number of reported cases presented by the response team is far below the reality in the country.

Concluding remarks

In this paper we propose the mathematical modeling and the dynamics of the new coronavirus (COVID-19) in which infectious individuals are divided into three subgroups representing three forms of infection in the population of the DRC. A rigorous mathematical analysis

of the proposed model was carried out. The sensitivity analysis of \mathcal{R}_0 with respect to the parameters of the system showed that in the order presented in Table 2, the parameters that most influence \mathcal{R}_0 are: $a, \beta, \rho_2, \rho_3, \rho_3$ and γ_1 .

Numerical simulations show that if control measures are not taken into account, COVID-19 will settle in the Congolese population. On the other hand, if the measures are taken into account, the pandemic will extinct in the future. Based on the results of our research, the information announced by the DRC health response team on the number of new cases per day is very low compared to reality. In fact, the team constantly gives the numbers of cases detected in relation to the available screening kits, which constitutes a capacity of less than 20% of screening capacity.

The model proposed in this paper, its mathematical analysis and the results obtained from the simulations are essential for the decision-makers in countries affected by COVID-19 in general and those of the

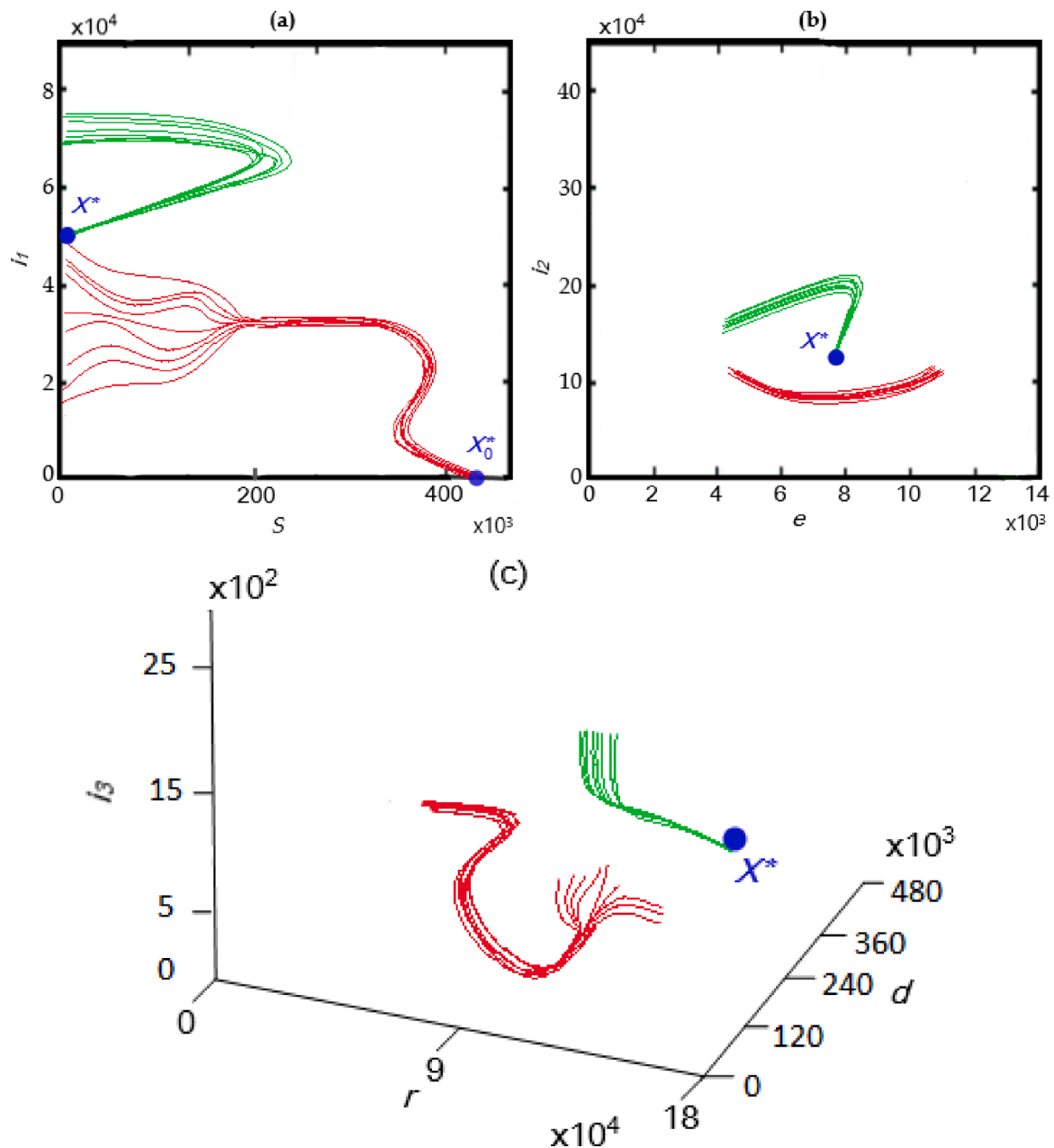


Fig. 9. (a), (b) and (c) show the dynamics of the global stability of DFE and the co-existing equilibrium for respectively different plans (i_1, s) , (i_2, e) and (i_3, r, d) .

DRC in particular in the sense that it gives a clear understanding of the spread of COVID-19 in the population and proposes the optimal control of the pandemic for its future extinction in the population.

As Africa in general and DRC in particular have a young population compared to Europe, and as the screening rate is low, the number of cases reported by the government remains low. The results of this paper therefore argue that many infected people assimilate their COVID-19 infection with other flu infection and treat themselves at home. This justifies the high prevalence obtained in our study compared to the values reported by the DRC response team. The government should consider the increasing of the capacity of COVID-19 screening and implement the control measures proposed here to significantly reduce the prevalence of this pandemic.

Availability of data and materials

Please contact authors for data and materials requests.

Funding

Not applicable.

Authors' contributions

AMN, SKK, SFB and KK wrote the first draft, investigated, proposed a methodology and did the data curation. AMN, SKK and SFB designed and analyzed the mathematical model. SKK, AMN and EFDG performed numerical simulations and data visualization. EFDG, KK and RBMN corrected and improved the final version. All authors read and approved the final draft.

Declaration of Competing Interest

The authors declare that they have no known competing financial interests or personal relationships that could have appeared to influence

the work reported in this paper.

Acknowledgements

The authors would like to thank the members of ABIL Research Center of the University of Kinshasa (www.abil.ac.cd) for material support that make this work more effective. They also thank Professor Taba Kalulu and Ir. Julio Nfundiko for the proofreading of this paper. AMN thanks the "Université Nouveaux Horizons" for the support in conducting this study. The authors express their deep thanks for the referee's valuable suggestions about the revision and improvement of the manuscript.

References

- [1] Booth TF, Kournikakis B, Bastien N, Ho J, Kobasa D, Stadnyk L, Li Y, Spence M, Paton S, Henry B, et al. Detection of airborne severe acute respiratory syndrome (SARS) coronavirus and environmental contamination in SARS outbreak units. *J Infectious Diseases* 2005;191:1472–7.
- [2] Bahl P, Doolan C, de Silva C, Chughtai AA, Bourouiba L, MacIntyre CR. Airborne or droplet precautions for health workers treating covid-19? *J Infect Dis* 2020.
- [3] Zhou F, Yu T, Du R, Fan G, Liu Y, Liu Z, Xiang J, Wang Y, Song B, Gu X, et al. Clinical course and risk factors for mortality of adult inpatients with covid-19 in Wuhan, China: a retrospective cohort study. *Lancet* 2020.
- [4] Gambaro F, Baidaliuk A, Behillil S, Donati F, Albert M, Alexandru A, Vanpeene M, Bizard M, Brisebarre A, Barbet M, et al., Introductions and early spread of SARS-CoV-2 in france, bioRxiv (2020).
- [5] Li H, Wang S, Zhong F, Bao W, Li Y, Liu L, Wang H, He Y, Age-dependent risks of incidence and mortality of covid-19 in hubei province and other parts of China 2, risk 31 (2020) 32.
- [6] Chen T, Wu D, Chen H, Yan W, Yang D, Chen G, Ma K, Xu D, Yu H, Wang H, et al. Clinical characteristics of 113 deceased patients with coronavirus disease 2019: retrospective study. *Bmj* 2020;368.
- [7] Cui S, Chen S, Li X, Liu S, Wang F. Prevalence of venous thromboembolism in patients with severe novel coronavirus pneumonia. *J Thromb Haemost* 2020.
- [8] Ferretti L, Wymant C, Kendall M, Zhao L, Nurtay A, Abeler-Dörner L, Parker M, Bonsall D, Fraser C. Quantifying SARS-CoV-2 transmission suggests epidemic control with digital contact tracing. *Science* 2020.
- [9] Liu Y, Yan L-M, Wan L, Xiang T-X, Le A, Liu J-M, Peiris M, Poon LL, Zhang W. Viral dynamics in mild and severe cases of covid-19. *Lancet Infect Dis* 2020.
- [10] He D, Zhao S, Lin Q, Zhuang Z, Cao P, Wang MH, Yang L. The relative transmissibility of asymptomatic cases among close contacts. *Int J Infectious Diseases* 2020.
- [11] W.H. Organization, et al., Coronavirus disease 2019 (covid-19): situation report, 72 (2020).
- [12] Kasereka S, Kasoro N, Chokki AP. A hybrid model for modeling the spread of epidemics: Theory and simulation, in. In: SKO-Maghreb: Concepts and Tools for knowledge Management (ISKO-Maghreb), 2014 4th International Symposium. IEEE; 2014. p. 1–7.
- [13] Kasereka S, Le Strat Y, Léon L. Estimation of infection force of hepatitis c virus among drug users in france. In: *Recent Advances in Nonlinear Dynamics and Synchronization*. Springer; 2018. p. 319–44.
- [14] Ndong A, Munganga J, Mwambakana J, Saad-Roy C, Van den Driessche P, Walo R. Analysis of a model of gambiense sleeping sickness in humans and cattle. *J Biological Dyn* 2016;10:347–65.
- [15] Goufo EFD, Maritz R, Munganga J. Some properties of the kermack-mckendrick epidemic model with fractional derivative and nonlinear incidence. *Adv Diff Eq* 2014;2014:278.
- [16] Ndong AM, Walo RO, Vala-kisisa MY. Optimal control of a model of gambiense sleeping sickness in humans and cattle, *American. J Appl Math* 2016;4:204–16.
- [17] Kasereka S, Goufo EFD, Tuong VH. Analysis and simulation of a mathematical model of tuberculosis transmission in democratic republic of the congo. *Adv Diff Eq* 2020;642:1–19.
- [18] Kasereka S, Goufo EFD, Tuong VH, Kyamakyia K, A stochastic agent-based model and simulation for controlling the spread of tuberculosis in a mixed population structure. In: *Developments of Artificial Intelligence Technologies in Computation and Robotics*, World Scientific, 2020b, pp. 659–666.
- [19] Nadim SS, Ghosh I, Chattopadhyay J, Short-term predictions and prevention strategies for covid-2019: A model based study, arXiv preprint arXiv:2003.08150 (2020).
- [20] Khan MA, Atangana A. Modeling the dynamics of novel coronavirus (2019-ncov) with fractional derivative. *Alexandria Eng J* 2020.
- [21] Resmawan R, Yahya L. Sensitivity analysis of mathematical model of coronavirus disease (covid-19) transmission. *CAUCHY* 2020;6:91–9.
- [22] Shah K, Abdeljawad T, Mahariq I, Jarad F. Qualitative analysis of a mathematical model in the time of covid-19. *BioMed Research Int* 2020;2020.
- [23] Thabet ST, Abdo MS, Shah K, Abdeljawad T. Study of transmission dynamics of covid-19 mathematical model under abc fractional order derivative. *Results Phys* 2020;19:103507.
- [24] Redhwan SS, Abdo MS, Shah K, Abdeljawad T, Dawood S, Abdo HA, Shaikh SL. Mathematical modeling for the outbreak of the coronavirus (covid-19) under fractional nonlocal operator. *Results Phys* 2020;19:103610.
- [25] Din RU, Shah K, Ahmad I, Abdeljawad T. Study of transmission dynamics of novel covid-19 by using mathematical model. *Adv Diff Eq* 2020;2020:1–13.
- [26] Zhang Z, Zeb A, Hussain S, Alzahrani E. Dynamics of covid-19 mathematical model with stochastic perturbation. *Adv Diff Eq* 2020;2020:1–12.
- [27] ud Din R, Seadawy AR, Shah K, Ullah A, Baleanu D, Study of global dynamics of covid-19 via a new mathematical model, *Results Phys* 19 (2020) 103468.
- [28] Van den Driessche P, Watmough J. Reproduction numbers and sub-threshold endemic equilibria for compartmental models of disease transmission. *Math Biosci* 2002;180:29–48.
- [29] Diekmann O, Heesterbeek JAP. *Mathematical epidemiology of infectious diseases: model building, analysis and interpretation*, volume 5. John Wiley & Sons; 2000.
- [30] Castillo-Chavez C, Song B. Dynamical models of tuberculosis and their applications. *Math Biosci Eng* 2004;1:361.
- [31] Flemming W, Rishel R, *Deterministic and stochastic optimal control* springer-verlag (1975).